Desalination and Water Treatment
www.deswater.com

doi: 10.5004/dwt.2021.27136

223 (2021) 316–327
May

A biodegradable based composite for wastewater treatment from cadmium and nickel ions

Aya H. Abdulghany[a], M.A. Abdel Khalek[a], Ghada A. Mahmoud[b,*], Hayam M. Ahmed[c], Yahya H.F. Al-Qudah[d]

[a]*Central Metallurgical Research and Development Institute (CMRDI), P.O. Box: 87, Helwan, Cairo, Egypt, emails: ayahussien32@gmail.com (A.H. Abdulghany), kalekma@yahoo.com (M.A. Abdel Khalek)*
[b]*National Center for Radiation Research and Technology, Atomic Energy Authority, P.O. Box: 29, Nasr City, Cairo, Egypt, Tel. +2-01065495895; Fax: +2-022 2749298; email: ghadancrrt@yahoo.com*
[c]*Faculty of Science, Al-Azhar University, Nasr City, Cairo 11371, Egypt, email: ha_ahmed@azher.edu.eg.com*
[d]*Al-Balqa Applied University, Zarka College, Zarka, Jordan, email: dr.yahyaqudah@gmail.com*

Received 20 July 2020; Accepted 27 January 2021

ABSTRACT

Cadmium and nickel ions were treated from wastewater by using (Chitosan/Gelatin/2-(Dimethylamino)ethyl methacrylate/silicon dioxide) composite (Cs/Gltn/PDMAEMA-SiO_2)comp that was performed by gamma irradiation. Chemical treatment of parent hydrogel (Cs/Gltn/PDMAEMA)gel was also done to introduce thiol groups in T-(Cs/Gltn/PDMAEMA). The characteristics of the composite compared with the parent and treated gels were examined by thermogravimetric analysis, X-ray diffraction, and field emission scanning electron microscopy. The adsorbent amount of the composite toward Cd^{2+} and Ni^{2+} was investigated. It was noticed that the maximum sorbent amount was performed at pH 5, 240 min contact time, and 10 g/L adsorbent dose. It can be also recognized that the sorption decreases as the temperature is increased. It is pointed to the exothermic adsorption character. The pseudo-second-order rate expression fits well the experimental data. The adsorption isotherm follows the Freundlich expression. The composite was tested for tenny wastewater treatment. It got a different trend from the obtained results indicated to some selectivity of this composite. The removal performance is 70% for heavy metal ions and 75% for color. The performance of other constituents is about 60%–70% except the turbidity is 46%.

Keywords: Adsorption; Composite; Hydrogel; Cation removal; Water treatment

1. Introduction

Heavy metals exist in the earth's crust. The random human activities changed the balance and they reach the drinking water supply [1]. The excessive amount can be detrimental to health. Cd can cause intoxications. Chronic exposure to Cd even in low concentrations could lead to anemia, anosmia (loss of sense of smell), cardiovascular diseases, renal damage, osteoporosis, fragile bones, hypertension, and lung damage. Cadmium exposure through pregnancy due to early birth and reduced weight [2]. Contact with nickel compounds can make unfavorable impacts on human health [3]. The reaction to nickel exposure is a skin rash that can produce allergic dermatitis. These serious impacts are caused by cadmium and nickel on human health. The WHO recommends 0.003 mg/L as the greatest level for Cd in water [4]. Also, EPA has since adopted the 0.1 mg/L as the greatest level for nickel in water

* Corresponding author.

supplies [5]. Thus, the removal of Cd and Ni ions from wastewaters has become an environmental necessity. Many methods are employed for excluding Cd and Ni ions. These include ion exchange, reverse osmosis, electrodialysis, precipitation, flocculation, and adsorption [6]. Adsorption has been seen to be preferred over other techniques due to low cost, flexibility, ease of design, and operation [7,8].

Hydrogel based on chitosan has a great interest in environmental biotechnology because it has high adsorption behavior toward heavy-metal ions, moreover, the low cost and it is simply prepared. The high numbers of $-NH_2$ and –OH groups included in the chitosan network increase the adsorption capacity [9]. However, the weak mechanical strength of chitosan-based materials limits their use as effective adsorbents [10]. The introduction of (PDMAEMA) to hydrogel provides environmental sensitivity and increases the mechanical properties. It is a water-soluble cationic polyelectrolyte having tertiary amino groups and it has a pKa of about 7.6 [11]. PDMAEMA contains a nitrogen atom that has the ability to complexation with different toxic heavy metal ions through coordination bond [12].

To promote adsorption efficiency, there are many different and unique nanoparticles utilized for entrapment in the hydrogel composite as hybrids [13,14]. SiO_2 is incorporated into the hydrogel matrix as it exhibits low toxicity and it is also environmentally inert [15].

In previous studies, Cs/Gltn/PDMAEMA/SiO_2 composite was produced by gamma irradiation for extraction of nitrate [16] and phosphate [17] anions. In this study, the prepared composite is characterized and utilized for the adsorption of Ni^{2+} and Cd^{2+}.

2. Materials and methods

2.1. Materials

Cs of medium molecular weight; the degree of deacetylation ~91% was received from Meron. (DMAEMA) of purity, 99.0% and SiO_2 were received from (Sigma-Aldrich, USA). Gelatin was supplied from El-Nasr Pharmaceutical Chemical-Prolabo (Cairo, Egypt). Additional chemicals are high grades and were bought from El-Nasr Co., (Cairo, Egypt).

2.2. Cs/Gltn/PDMAEMA/SiO_2 composite synthesis

0.03 g of SiO_2 powder was added to 99 mL of deionized water and 1 mL acetic acid then it was sonicated for 30 min. 1.5 g of Cs was added and stirred for 1 h at 60°C in the water bath. 20 g of gelatin was dissolved in 100 mL of deionized water at 60°C for 30 min in the water bath. The two solutions were incorporated and DMAEMA of concentration 0.36 (g/g) was added to the solution where the total concentration was 20 wt.%. The solution mixture was transferred into vials and was irradiated at an irradiation dose of 15 kGy. ^{60}Co gamma source installed at the National Centre for Radiation Research and Technology (NCRRT), Egypt. After irradiation, the formed composite cylinder was cut into discs. All specimens were extracted in distilled water at 80°C for 2 h to exclude the un-reacted materials then, air-dried to a constant weight.

2.3. Treated Cs/Gltn/PDMAEMA hydrogel synthesis

(Cs/Gltn/PDMAEMA)gel was prepared by following the same steps of Cs/Gltn/PDMAEMA/SiO_2 composite synthesis without adding SiO_2. In a one-neck flask, 15 g of Cs/Gltn/PDMAEMA hydrogel, 15 g thiourea, 50 mL HCl, and 150 mL H_2O were combined and stirred for 24 h [18]. After that, the swelled hydrogel was transferred to another flask containing 10% (w/v) NaOH and stirred for 6 h. The hydrogel was washed with acetone, ethanol, and deionized water to remove excess agents and then dried at 50°C.

2.4. Instrumentations

The thermogravimetric analysis (TGA) study was taken out on Shimadzu-30 (TGA-30, Kayto, Japan) at a heating rate of 10°C/min in a temperature range from ambient to 500°C.

The surface morphology was investigated using the field emission scanning electron microscope (QVANTA FEG 250, Netherlands) at an acceleration voltage of 20 kV.

X-ray diffraction (XRD) analysis was performed using X-ray automatic powder diffraction system Cu kα λ = 1.5 Å radiation. A Philips PW 1730 powder X-ray diffractometer (Holland) was used for this purpose.

2.5. Adsorption study

Adsorption examinations were made by the batch equilibration technique in duplicate. The metal ion determination of nickel and cadmium was done using atomic absorption spectroscopy (Perkin Elmer, Model A Analyst 200, USA). The influence of contact time was investigated in the period of 15–180 min using 20 mg/L of metal ion initial concentration and 0.05 g of the sample ambient temperature in a mechanical shaker having 120 rpm. The pH effect was done by adjusting the pH using 0.1 mol/L HCl and NaOH. The dosage effect was done by using doses between 0.05 and 0.3 g/L. The temperature effect was done in the range of 30°C–60°C. The effect of initial concentration was studied using the concentrations from 20.5 to 102 mg/L for Cd^{2+} ions and 21.5 to 107 mg/L for Ni^{2+} ions. The adsorption amount (q_e, mg/g) and the removal percentage for these ions were calculated by Eqs. (1) and (2), respectively [19].

$$q_e = \frac{\left(C_0 - C_e\right)V}{M} \tag{1}$$

$$\text{Removal}\left(\%\right) = \frac{C_0 - C_e}{C_0} \times 100 \tag{2}$$

where C_0 (mg/L) is the initial concentration of the solution. C_e (mg/L) is the equilibrium concentration after the adsorption procedure. V (L) is the solution volume. M (g) is the adsorbent weight.

2.6. Application on a real wastewater

Wastewater from the tannery industry that contains heavy metal ions, coloring materials, and other pollutants was employed in this study. A 0.2 g of the sample was

immersed in 100 mL of effluent for 6 h at ambient temperature. The analysis of the wastewater before and after treatment was done.

2.7. Evaluation of industrial wastewater

Chemical oxygen demand (COD) and biochemical oxygen demand (BOD) were investigated using the respirometric method. The sample is connected to a pressure sensor in an isolated system. BOD test was performed in 5 d period in airtight bottle under temperature (20°C ± 1°C) and in the absence of any light to prevent photosynthesis.

total solid (TS), total suspended solid (TSS), and heavy metals were measured according to Standard Methods [20]. Total solids are evaluated by evaporating water out of the sample and weighing the solid. TSS was determined by turbidity meter, HI 93703, microprocessor.

3. Results and discussion

3.1. Thermo-gravimetric analysis

TGA derivative thermograms of (Cs/Gltn/PDMAEMA) gel, T-(Cs/Gltn/PDMAEMA), and (Cs/Gltn/PDMAEMA/SiO_2)comp are presented in Fig. 1. The obtained data are shown in Table 1. The thermogram of (Cs/Gltn/PDMAEMA) gel showed three decomposition stages. The first decomposition stage between 52°C and 131°C is attributed to the vaporization of the unbonded water. The second decomposition stage between ~174°C and 362°C could be explained by the degradation and depolymerization of the hydrogel. The third decomposition stage between ~524°C and 578°C as a result of oxidative decomposition of the residues [21]. Three endothermic peaks centered at 102°C, 260°C, and 252°C, respectively, characterized these decomposition stages. For T-(Cs/Gltn/PDMAEMA), two decomposition stages were observed, the first decomposition stage at ~411°C–465°C due to degradation of the backbone matrix. The second decomposition stage at 613°C–669°C due to the complete decomposition of the residues. These decomposition stages characterized by two endothermic peaks centered at 452°C and 631°C, respectively. More stability up to 400°C was observed which means the higher thermal stability of the treated gel than the hydrogel. For the (Cs/Gltn/PDMAEMA-SiO_2)comp, the first decomposition stage occurs gradually in the temperatures range of ~91°C–318°C. It suggested the rigid structure and indicated the thermal stability. The second weight loss occurring in the temperature range of 465°C–686°C. It was due to the decomposition of the organic moiety and the dehydroxylation of silanol groups [22]. Two endothermic peaks centered at 198°C and 583°C accompanied the decomposition stages.

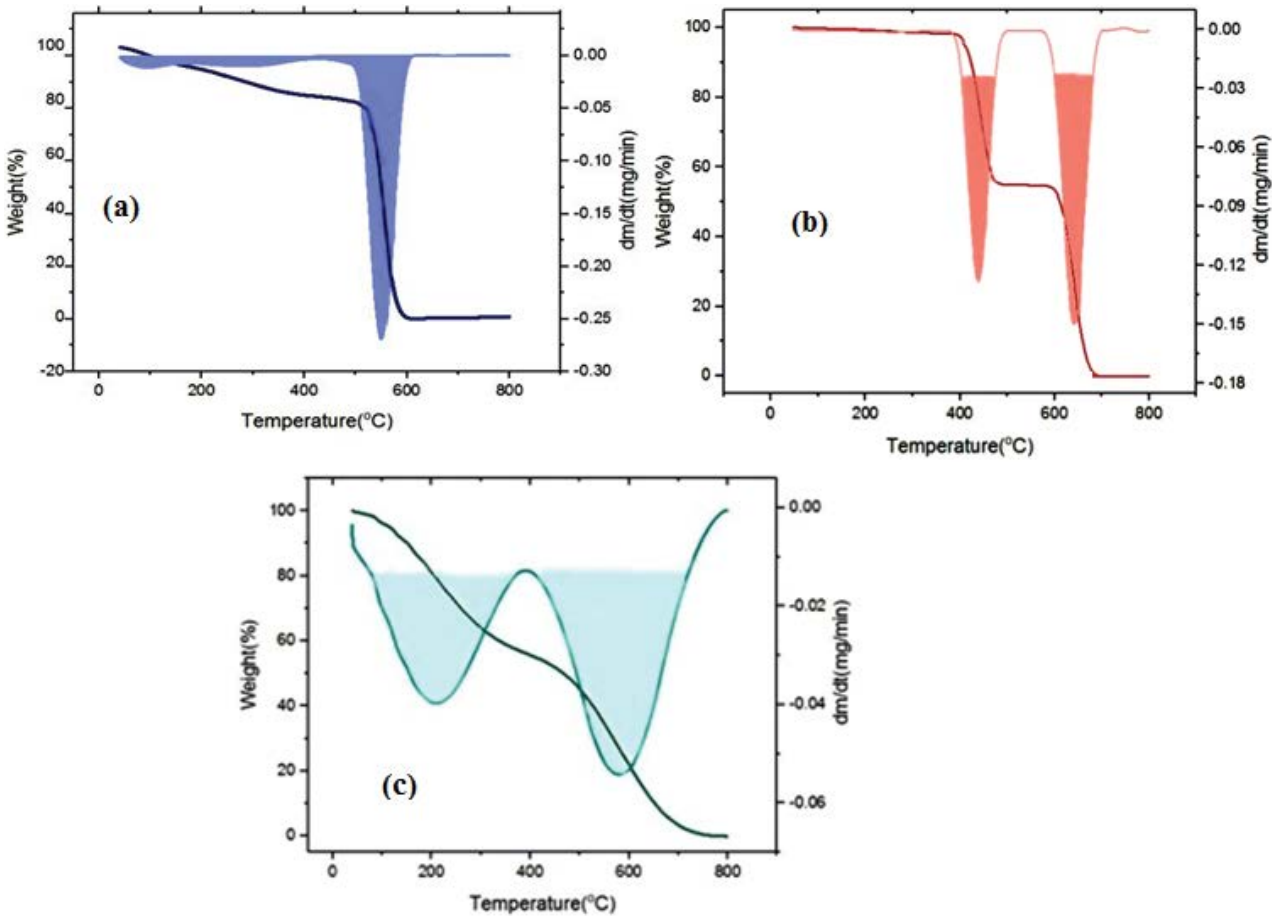

Fig. 1. TGA thermograms of (Cs/Gltn/PDMAEMA)gel (a), T-(Cs/Gltn/PDMAEMA) (b), and (Cs/Gltn/PDMAEMA-SiO_2)comp.

Table 1
TGA data for the thermal degradation of (Cs/Gltn/PDMAEMA), T-(Gltn/PDMAEMA), and (Cs/Gltn/PDMAEMA/SiO_2)

Sample	Stage	Onset (°C)	Endset (°C)	Weight loss (%)	Residue (%)
(Cs/Gltn/PDMAEMA)	1	51.8	130.7	5.59	15.46
	2	174.3	361.7	10.04	
	3	524.4	578.1	68.91	
T-(Gltn/PDMAEMA)	1	411.4	464.6	38.8	14.00
	2	612.9	669.1	47.2	
(Cs/Gltn/PDMAEMA/SiO_2)	1	91.3	318	37.06	15.30
	2	465.6	686.7	47.3	

3.2. XRD analysis

Fig. 2 shows XRD patterns of (Cs/Gltn/PDMAEMA) gel, T-(Cs/Gltn/PDMAEMA), and (Cs/Gltn/PDMAEMA-SiO_2)comp. The XRD patterns of (Cs/Gltn/PDMAEMA) gel and T-(Cs/Gltn/PDMAEMA) exhibit amorphous broad peaks at 2θ = 18.22° and 17.04°, respectively. For (Cs/Gltn/PDMAEMA-SiO_2)comp, a sharp peak appeared at 2θ = 21.6° and a weak peak was observed at 2θ = 26.8°. The crystalline phase confirmed the crystalline structure of silica particles [23]. The appearance of crystalline characteristics suggested that the preparation method did not include a chemical reaction, and just a physical modification occurred on the particles. The silica interacts with the glucopyranose ring in chitosan through hydrogen-bonding interactions [24].

3.3. Field emission scanning electron microscopy

Fig. 3 shows the FESEM images of the (Cs/Gltn/PDMAEMA)gel, T-(Cs/Gltn/PDMAEMA), and (Cs/Gltn/PDMAEMA-SiO_2)comp. As obtained in Fig. 3a, the (Cs/Gltn/PDMAEMA)gel appears as a coarse surface with some protrusions. For T-(Cs/Gltn/PDMAEMA), Fig. 3b, some surface flattening was obtained as a result of treatment. In (Cs/Gltn/PDMAEMA-SiO_2)comp, Fig. 3c, the surface exhibits some protuberances and is covered by the nearly small spherical shiny spots of silica. It was noted that no agglomeration was observed which indicates the great dispersion of silica in the matrix. Moreover of some smoothness in the surface was done by adding silica in the matrix compared with the pure hydrogel. This explained that the SiO_2 was strongly incorporated in the composite matrix.

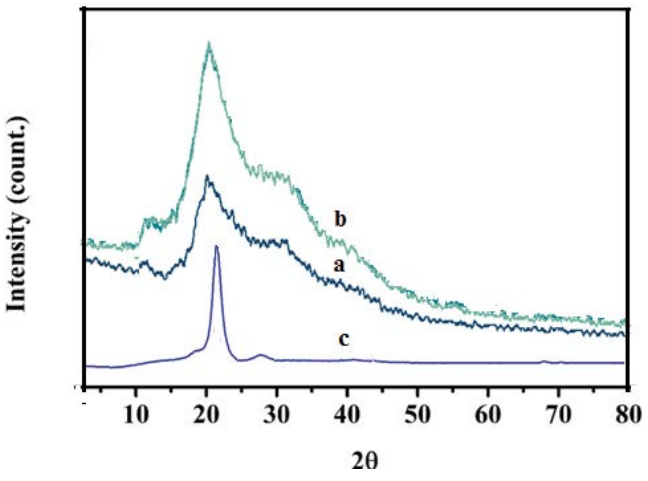

Fig. 2. XRD patterns of (Cs/Gltn/PDMAEMA)gel (a), T-(Cs/Gltn/PDMAEMA) (b), and (Cs/Gltn/PDMAEMA-SiO_2)comp.

3.4. Adsorption study

The adsorption of Cd^{2+} and Ni^{2+} from aqueous solutions by (Cs/Gltn/PDMAEMA-SiO_2)comp and T-(Cs/Gltn/PDMAEMA) compared to(Cs/Gltn/PDMAEMA)gel are studied. Effects of pH, contact time, initial concentration, the dosage of sorbent, and temperature on the sorption have been investigated.

3.4.1. Effect of pH

The adsorption of Cd^{2+} and Ni^{2+} by (Cs/Gltn/PDMAEMA)gel, T-(Cs/Gltn/PDMAEMA), and (Cs/Gltn/PDMAEMA-SiO_2)comp at various pHs is shown in Fig. 4. It can be noted that the sorption strength increases with rising in pH value of Cd^{2+} and Ni^{2+} media up to the maximum value at pH = 5 above this value a drop is done. The weak adsorption at lower pHs is due to the partial protonation of the active groups which leads to generating partially positive sites such as ($–NH^{3+}$/$–NH^{2+}(CH_3)_2$/$–SH^{2+}$ and $–Si–OH_2^+$). It is responsible for decreasing the affinity toward the metal ions by the electrostatic repulsion of the positively charged moieties. Moreover, the competition of H^+ with Cd^{2+} or Ni^{2+} for the occupying of adsorption sites is very strong [25]. As the pH increases, the free lone pair of electrons on nitrogen, oxygen, and sulfur atoms are suitable for coordination with metal ions [26]. Moreover, the availability of the ionic interaction between the carboxylate groups and Cd^{2+} or Ni^{2+} [27] is responsible for the higher removal affinity. Above pH 5, the precipitation of the metal ions as metal hydroxide causes the drop of adsorption [28]. The affinity of sorbents to Ni^{2+} is higher than Cd^{2+} ions. It suggested the possible selectivity toward Ni^{2+}. The smaller ionic size for Ni^{2+} ions relative to Cd^{2+} ions may be the reason for this behavior. The large ionic radius of Cd^{2+} (0.92 Å) compared with Ni^{2+} (0.70 Å) induced a quick saturation of the active sites by the steric overcrowding thus the surface available for Ni^{2+} ions become larger than for Cd^{2+} [25]. On the other hand, (Cs/Gltn/PDMAEMA-SiO_2)comp has the highest value of adsorption capacity. It has the highest number of functional groups

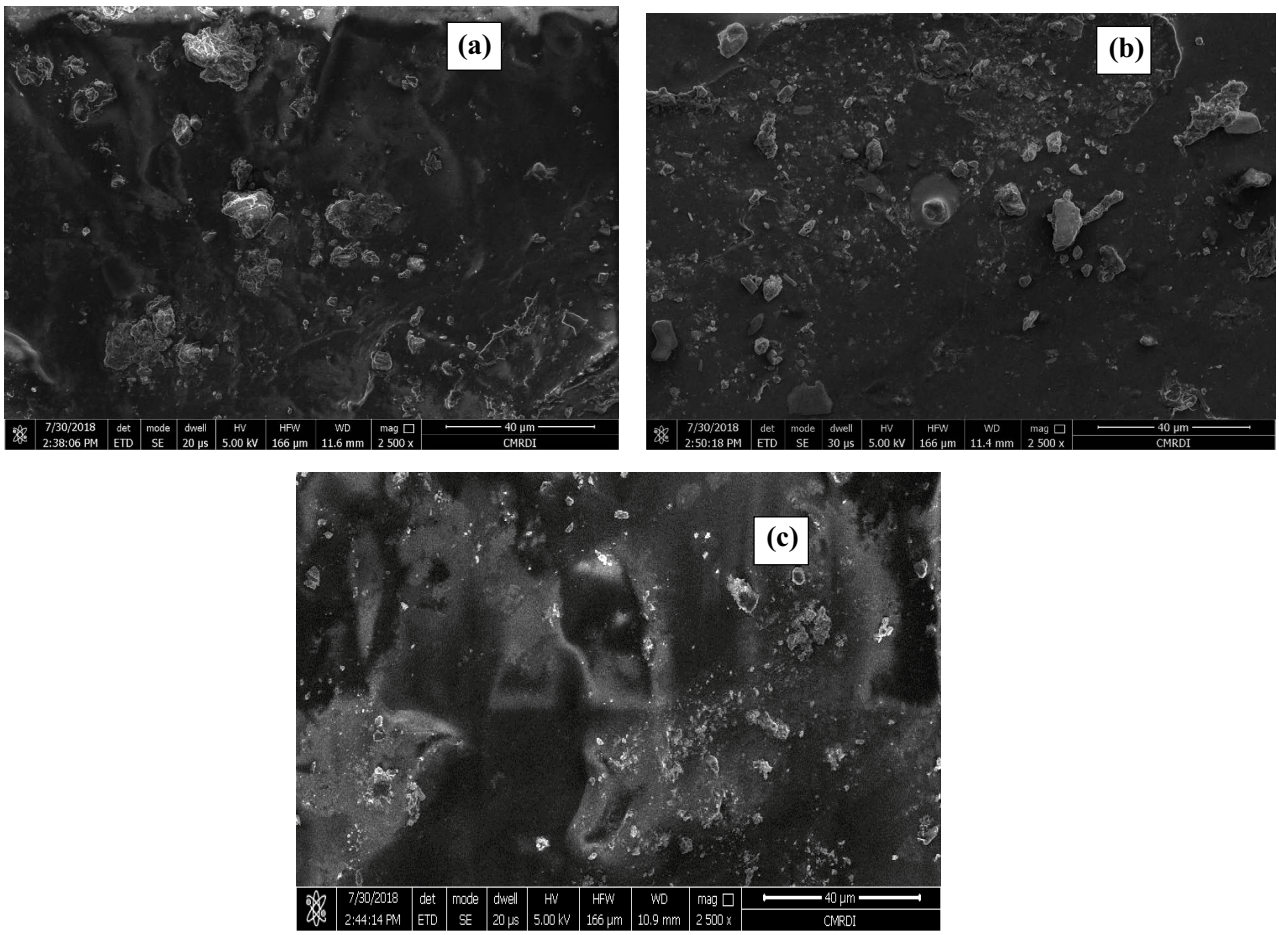

Fig. 3. FESEM images of (Cs/Gltn/PDMAEMA)gel (a), T-(Cs/Gltn/PDMAEMA) (b), and (Cs/Gltn/PDMAEMA-SiO_2)comp.

that cause the affinity toward Ni^{2+} and Cd^{2+}. The effect of the presence of SiO_2 in the composite is presented in Fig. 5.

3.4.2. Effect of treatment time

Effect of contact time on the adsorption of Cd^{2+} and Ni^{2+} by (Cs/Gltn/PDMAEMA)gel, T-(Cs/Gltn/PDMAEMA), and (Cs/Gltn/PDMAEMA-SiO_2)comp was investigated as presented in Fig. 6. The adsorption of Cd^{2+} and Ni^{2+} enhances with expanding the contact time for all investigated systems. The adsorption rate is accelerated in the first hour but becomes slower until equilibrium within approximately 240 min. The beginning high adsorption rate probably results from the high availability of active positions on the surface [29].

3.4.3. Effect of initial concentration

The influence of initial concentration on the adsorption of Cd^{2+} and Ni^{2+} cations by (Cs/Gltn/PDMAEMA)gel, T-(Cs/Gltn/PDMAEMA), and (Cs/Gltn/PDMAEMA-SiO_2) comp was investigated as presented in Fig. 7. The sorption capacity significantly improves as the original concentration of these cations is increased. This assigned to the development of interaction probability of adsorbate ions with adsorption positions on the adsorbent surface [30]. However, the removal percentage of these cations decreases by raising the initial concentration. At higher concentrations, the capacity of the adsorbent nears saturation, thus, a reduction of the overall removal (%) [31].

3.4.4. Effect of adsorbent dose

The influence of adsorbent dose on the adsorption of Cd^{2+} and Ni^{2+} by (Cs/Gltn/PDMAEMA)gel, T-(Cs/Gltn/PDMAEMA), and (Cs/Gltn/PDMAEMA-SiO_2)comp is presented in Fig. 8. The sorption capacity decreases as the dosage is increased from 0.05 to 0.3 g/20 mL (2.5–15 g/L). This is because of the incomplete exploitation of the free active positions for adsorption at higher adsorbent dosage in comparison to the lower adsorbent dosage [32]. However, the removal of these cations improves as the dosage is increased. Because there are high available active sites that enhanced the removal [33]. A little progress in adsorption is done by raising the dose from 0.2 to 0.3 g/20 mL. This means from the economical point of view the optimum sorbent dosage is 0.2 g/20 mL corresponding to 10 g/L.

3.4.5. Effect of temperature

The influence of temperature on the adsorption of Cd^{2+} and Ni^{2+} by (Cs/Gltn/PDMAEMA)gel, T-(Cs/Gltn/PDMAEMA), and (Cs/Gltn/PDMAEMA-SiO_2)comp is

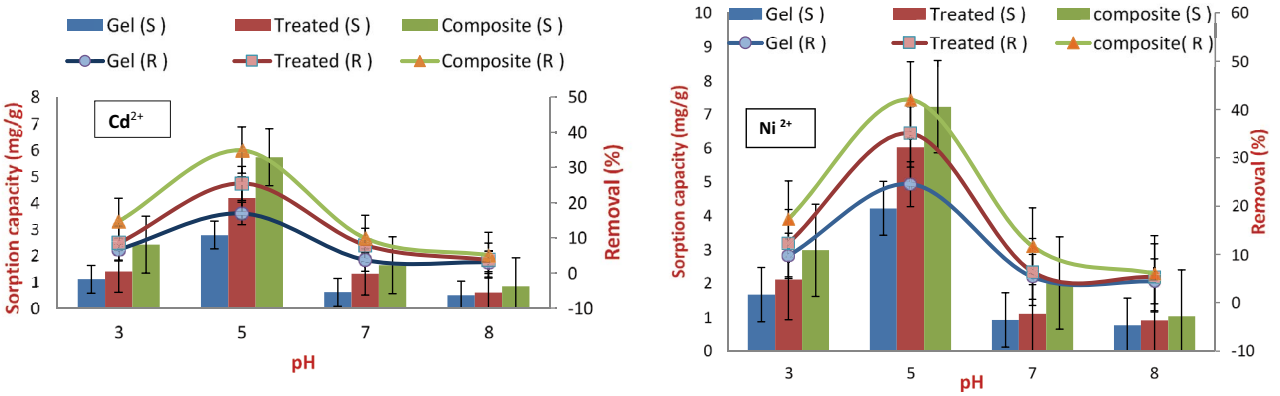

Fig. 4. Effect of pH on the adsorption capacity and removal percent of Cd^{2+} and Ni^{2+} by (Cs/Gltn/PDMAEMA)gel, T-(Cs/Gltn/PDMAEMA), and (Cs/Gltn/PDMAEMA-SiO_2)comp at ambient temperature, time; 240 min, initial concentration 41 and 43 mg/L for Cd^{2+} and Ni^{2+}, respectively, and adsorbent dose; 2.5 g/L.

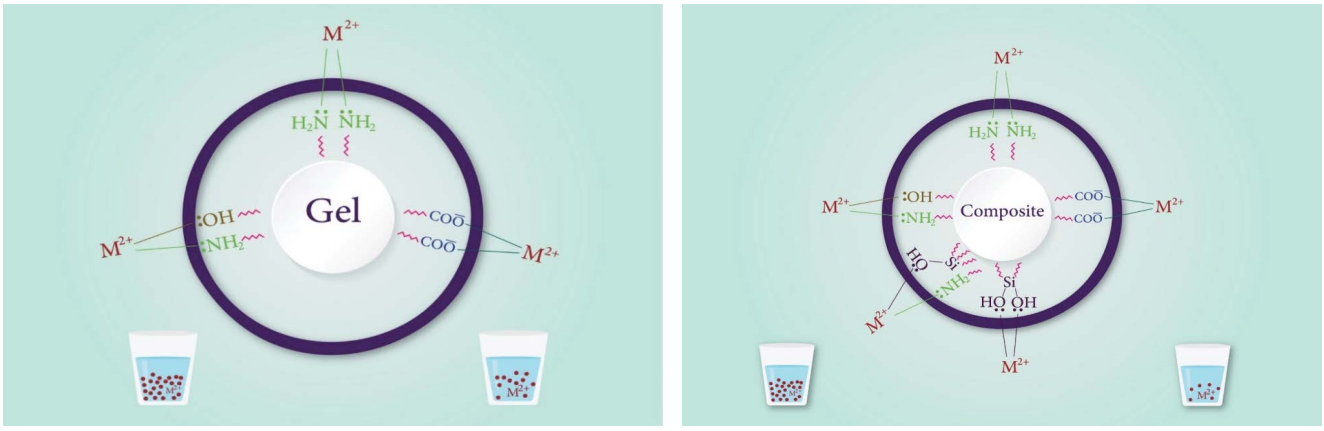

Fig. 5. A diagram presents the effect of the presence of SiO_2 in (Cs/Gltn/PDMAEMA-SiO_2)comp on the metal ions adsorption (M^{2+}:Cd^{2+} and Ni^{2+}).

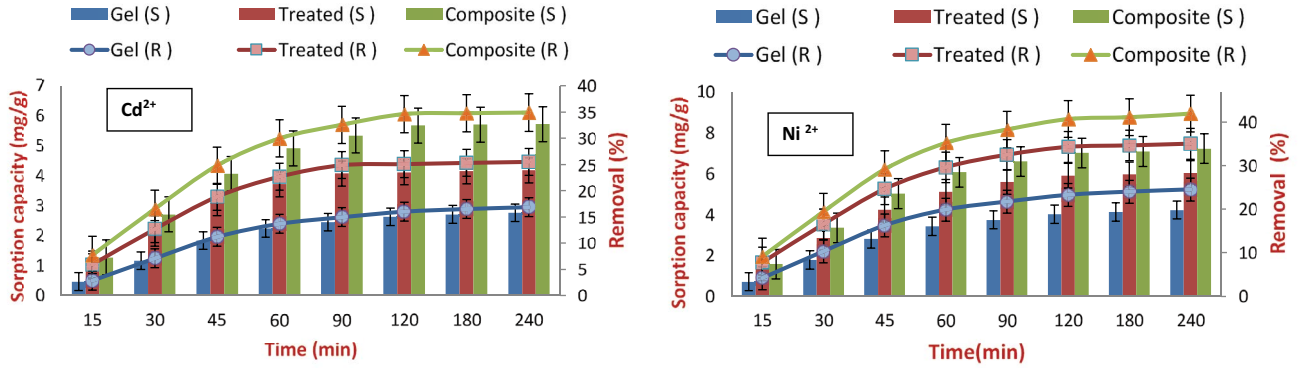

Fig. 6. Effect of time on the adsorption capacity and removal percent of Cd^{2+} and Ni^{2+} (Cs/Gltn/PDMAEMA)gel, T-(Cs/Gltn/PDMAEMA), and (Cs/Gltn/PDMAEMA-SiO_2)comp at ambient temperature, pH; 5, initial concentration; 41 and 43 mg/L for Cd^{2+} and Ni^{2+}, respectively, and adsorbent dose; 2.5 g/L.

presented in Fig. 9. The sorption decreases as the temperature is increased. The destruction of the effective binding position of the adsorbent and the tendency of desorption may responsible for the decline of sorption [34]. This result indicated the exothermic behavior of the adsorption of all investigated systems.

3.4.6. Adsorption kinetics

The adsorption kinetics by (Cs/Gltn/PDMAEMA)gel, T-(Cs/Gltn/PDMAEMA), and (Cs/Gltn/PDMAEMA-SiO_2) comp were tested using pseudo-first-order (Eq. (3)) and pseudo-second-order (Eq. (4)) kinetic rate expressions [35]:

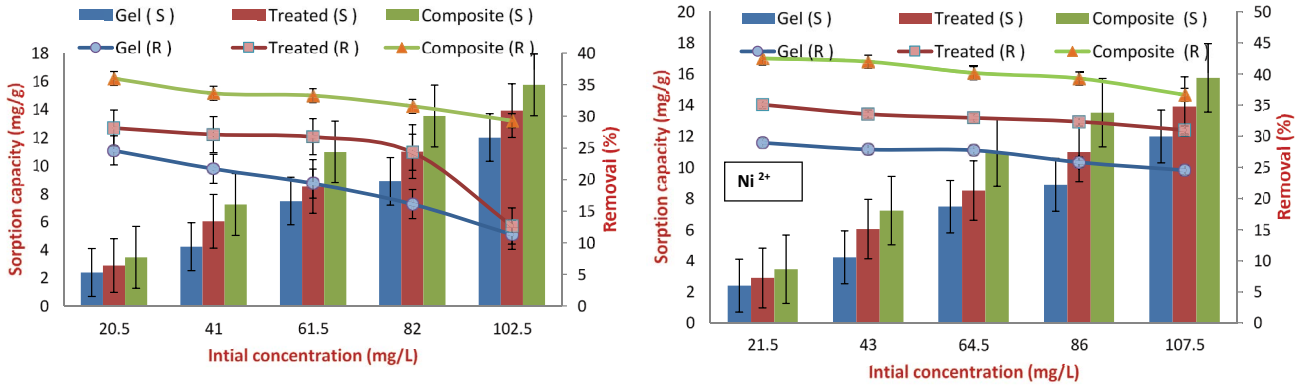

Fig. 7. Effect of initial concentration on adsorption capacity and removal percent of Cd^{2+} and Ni^{2+} by Cs/Gltn/PDMAEMA)gel, T-(Cs/Gltn/PDMAEMA), and (Cs/Gltn/PDMAEMA-SiO_2) comp at ambient temperature, time; 240 min, pH; 5 and adsorbent dose; 2.5 g/L.

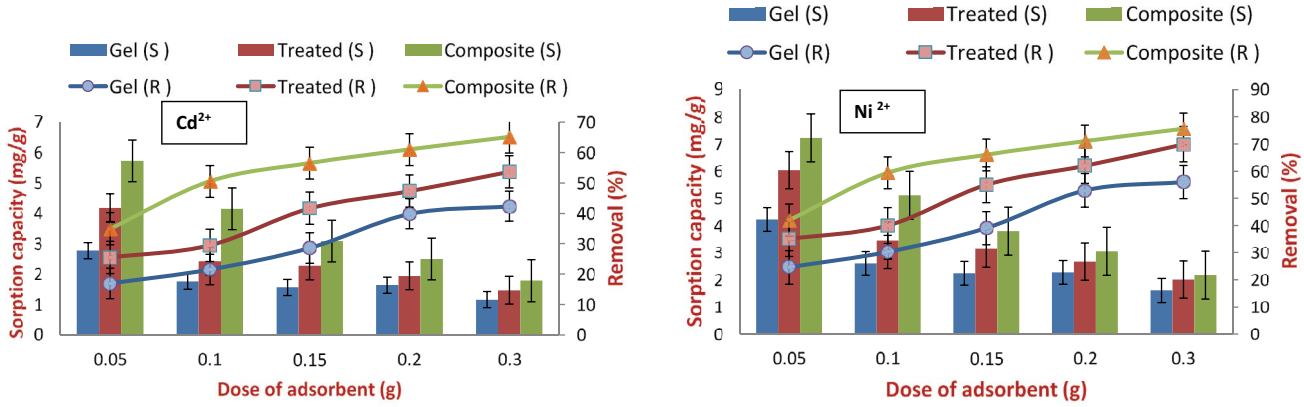

Fig. 8. Effect of adsorbent dose on the adsorption capacity and removal percent of Cd^{2+} and Ni^{2+} by Cs/Gltn/PDMAEMA)gel, T-(Cs/Gltn/PDMAEMA), and (Cs/Gltn/PDMAEMA-SiO_2)comp at time; 240 min, pH; 5 and initial concentration 41 and 43 mg/L for Cd^{2+} and Ni^{2+}, respectively.

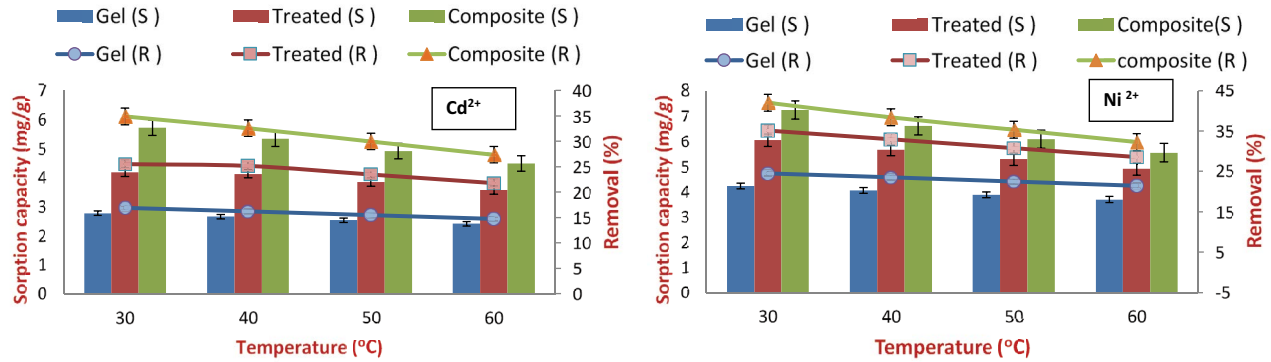

Fig. 9. Effect of temperature on the adsorption capacity and removal percent of Cd^{2+} and Ni^{2+} by Cs/Gltn/PDMAEMA)gel, T-(Cs/Gltn/PDMAEMA), and (Cs/Gltn/PDMAEMA-SiO_2)comp at time; 240 min, initial concentration; 41 and 43 mg/L for Cd^{2+} and Ni^{2+}, respectively, pH; 5, adsorbent dose; 2.5 g/L.

$$\log\left(q_e - q_t\right) = \log q_e - \frac{k_1}{2.303}t \tag{3}$$

$$\frac{t}{q_t} = \frac{1}{k_2 q_e^2} + \frac{1}{q_e}t \tag{4}$$

where q_e (mg/g) and q_t (mg/g) are the amount of adsorbed cations at equilibrium and at different time intervals, respectively. k_1 (1/min) is the pseudo-first-order rate constant. k_2 (g/mg min) is the pseudo-second-order rate constant.

The linear-form plots of the two expressions are presented in Figs. 10 and 11. The lines for pseudo-second-order

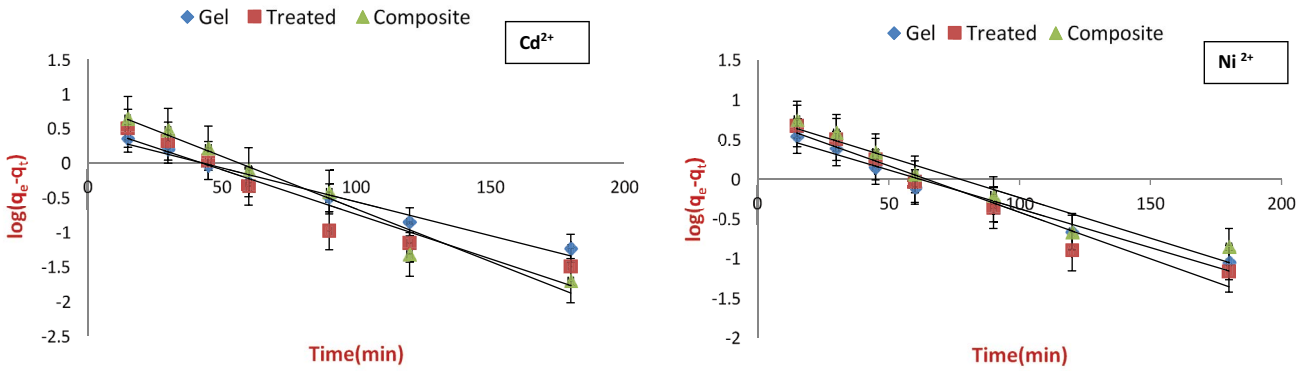

Fig. 10. Curve fitting the pseudo-first-order model for Cd^{2+} and Ni^{2+} ions by (Cs/Gltn/PDMAEMA)gel, T-(Cs/Gltn/PDMAEMA), and (Cs/Gltn/PDMAEMA-SiO_2)comp.

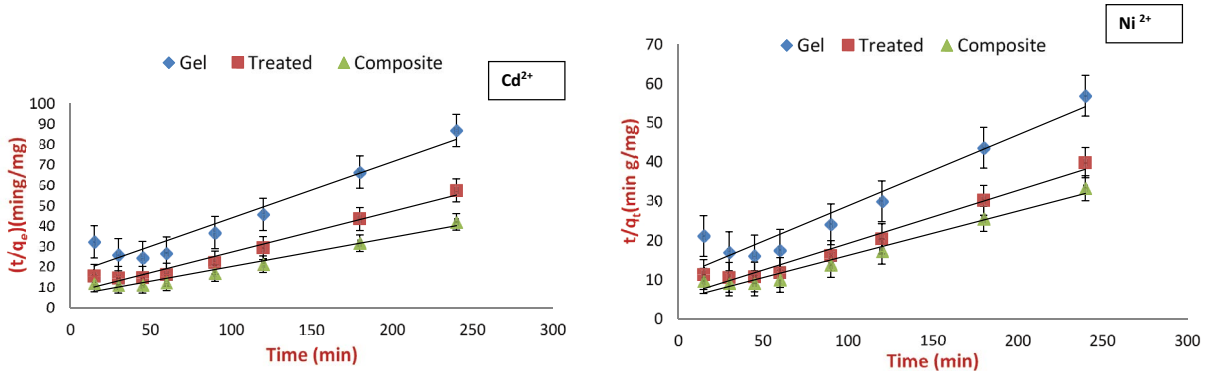

Fig. 11. Curve fitting the pseudo-second-order model for Cd^{2+} and Ni^{2+} by (Cs/Gltn/PDMAEMA)gel, T-(Cs/Gltn/PDMAEMA), and (Cs/Gltn/PDMAEMA-SiO_2)comp.

kinetic rate expression have higher R^2 than the pseudo-first-order kinetic rate expression as presented in Table 2. This means the pseudo-second-order rate expression fit well the experimental data; therefore, a chemical reaction may be included in the process.

3.4.7. Adsorption isotherms

3.4.7.1. Langmuir isotherm model

This design suggests monolayer adsorption happening at definite localized places [36]. The linear form of the Langmuir model, represented by Eq. (5):

$$\frac{C_e}{q_e} = \frac{C_e}{q_{\max}} + \frac{1}{bq_{\max}} \tag{5}$$

where C_e (mg/L) is the concentration at the equilibrium. q_e (mg/g) is the amount adsorbed at equilibrium. b (L/g) the Langmuir isotherm constant. $q_{\max}$ (mg/g) the maximum adsorption capacity.

The isotherm plots of Langmuir model for uptake of Cd^{2+} and Ni^{2+} by (Cs/Gltn/PDMAEMA)gel, T-(Cs/Gltn/PDMAEMA), and (Cs/Gltn/PDMAEMA-SiO_2)comp is shown in Fig. 12. The obtained data are reviewed in Table 3. The relatively low values of R^2 got from the Langmuir isotherm showed the appropriateness of the employment of this model to all systems. The Langmuir isotherm does not fit well the experimental adsorption data. This suggests that the sorption is not characterized by chemical nature.

3.4.7.2. Freundlich isotherm model

The Freundlich isotherm is applied for heterogeneous systems, as well as, multilayer sorption (Eq. (6)). The linear form of the model represented by Eq. (7) [37].

$$q_e = K_F C_e^{1/n} \tag{6}$$

$$\ln q_e = \ln K_F + \frac{1}{n}\ln C_e \tag{7}$$

where q_e is the adsorbed amount per unit weight of sorbent at equilibrium (mg/g). C_e corresponds to the residual concentration at equilibrium (mg/L). K_F is the sorption capacity (mg/g). n is the sorption intensity (unit less). n indicates the favorability of the adsorption. If n values higher than 1 the adsorption is favorable [38]. The values of K_F and $1/n$ are by plotting $\ln q_e$ as a function of $\ln C_e$, Fig. 13 and the obtained data is shown in Table 3. The Freundlich isotherm model showed a good fit for experimental adsorption data. The values of R^2 got from the Freundlich isotherm equation are close to unity. It indicated the appropriateness of

Table 2
Pseudo-first-order and pseudo-second-order kinetic parameters for adsorption of Cd^{2+} and Ni^{2+} ions by (Cs/Gltn/PDMAEMA), T-(Gltn/PDMAEMA), and (Cs/Gltn/PDMAEMA/SiO_2)

Items	Cs/Gltn/PDMAEMA		T-(Cs/Gltn/PDMAEMA)		Cs/Gltn/PDMAEMA/SiO_2	
	Cd^{2+}	Ni^{2+}	Cd^{2+}	Ni^{2+}	Cd^{2+}	Ni^{2+}
$q_{e,exp}$ (mg/g)	2.77	4.20	4.18	6.03	5.72	7.22
Pseudo-first-order model						
R^2	0.93	0.93	0.92	0.96	0.96	0.94
k_1 (min^{-1})	–0.02	–102.04	–0.03	–84.75	–0.04	–98.04
$q_{e,cal}$ (mg/g)	2.6539	4.0476	3.5768	5.7916	7.3468	6.25
Pseudo-second-order model						
R^2	0.9746	0.9706	0.9667	0.9673	0.9651	0.97
k_2 (g mg^{-1} min^{-1})	0.0046	0.0030	0.0056	0.0032	0.0035	0.0026
$q_{e,cal}$ (mg/g)	3.63	5.53	5.01	7.37	6.99	8.86

Table 3
Langmuir and Freundlich models constants for Cd^{2+} and Ni^{2+} ions adsorption

Items	Cs/Gltn/PDMAEMA		T-(Cs/Gltn/PDMAEMA)		Cs/Gltn/PDMAEMA/SiO_2)	
	Cd^{2+}	Ni^{2+}	Cd^{2+}	Ni^{2+}	Cd^{2+}	Ni^{2+}
Langmuir model						
R^2	0.36	0.50	0.89	0.85	0.75	0.74
$q_{max',cal}$ (mg/g)	80.65	285.71	52.08	97.09	72.99	70.92
$q_{max',exp}$ (mg/g)	10.57	11.99	12.11	13.90	13.59	15.75
b (L/mg)	0.0018	0.0005	0.004	0.0022	0.0038	0.0044
Freundlich model						
R^2	0.99	0.988	0.99	0.998	0.99	0.988
n	1.086	1.028	1.141	1.074	1.107	1.109
K_F (mg/g)	0.179	0.164	0.277	0.254	0.339	0.378

the application of this model to all systems. The adsorption process occurred mainly by the opposite charge attraction (physical adsorption).

3.5. Thermodynamic study

Enthalpy change ($\Delta H°$) and entropy change ($\Delta S°$) of the adsorption can be calculated by the following equation [16]:

$$\ln k = \frac{\Delta S°}{R} - \frac{\Delta H°}{RT} \quad (8)$$

where k = Fe/(1 – Fe), and Fe = $(C_0 - C_e)/C_0$, T (K) is the temperature, and R is the gas constant (8.314 J/mol K). $\Delta H°$ and $\Delta S°$ have been evaluated from Fig. 14 and the summarized analyzed data is shown in Table 4.

It was found that the values of $\Delta H°$ are negative for all investigated systems and they are lower than 40 kJ/mol which indicated the sorption is exothermic physisorption and not favorable at higher temperatures. The negative values of $\Delta S°$ refracted a random decrease at the solid/liquid interface during the adsorption.

3.6. Application on real wastewater

The composite was tested for the processing of real wastewater. Characterization was performed before and after treatment under the optimum adsorption conditions as got in Table 5. The efficiency is 70% and 75% for heavy metal ions and color, respectively. The efficiency of other constituents is between 60% and 70% except the turbidity is 46%. This means the composite is not a specific adsorbent for the insoluble materials. Table 6 presents the chemical analysis before and after treatment. The removal is found to be arranged in sequence of Cd^{2+} > Cu^{2+} > Pb^{2+} > Ni^{2+} > Zn^{2+} > As^{3+} > Cr^{3+}. The lowest removal percentage is 66% for chromium ions (from 152 to 51 mg/L). The highest removal percentage is about 89% for cadmium ions (from 8 to 0.89 mg/L). The trend is different from our experimental trend for Cd^{2+} and Ni^{2+}. The top controlled parameter on the adsorption might be the initial concentration

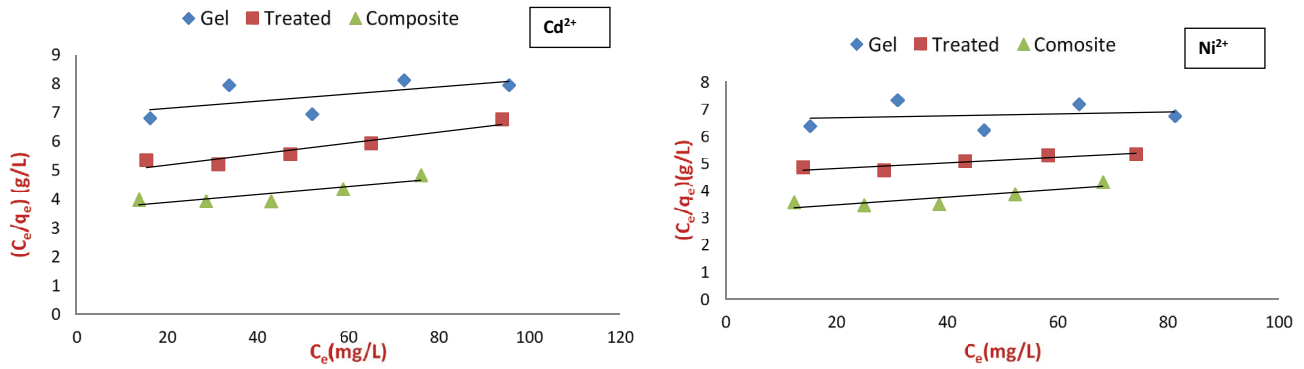

Fig. 12. Langmuir adsorption isotherm of Cd^{2+} and Ni^{2+} ions by (Cs/Gltn/PDMAEMA)gel, T-(Cs/Gltn/PDMAEMA), and (Cs/Gltn/PDMAEMA-SiO_2)comp.

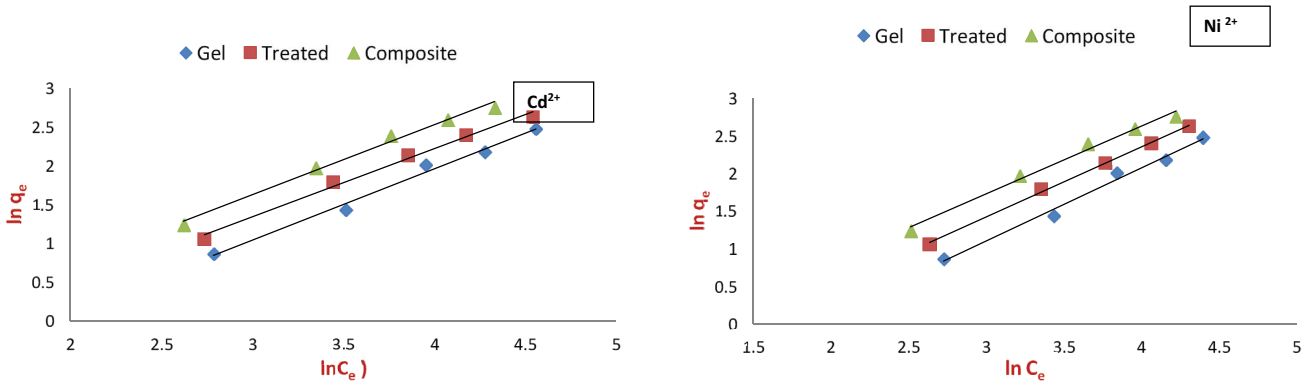

Fig. 13. Freundlich adsorption isotherm of Cd^{2+} and Ni^{2+} ions by (Cs/Gltn/PDMAEMA)gel, T-(Cs/Gltn/PDMAEMA), and (Cs/Gltn/PDMAEMA-SiO_2)comp.

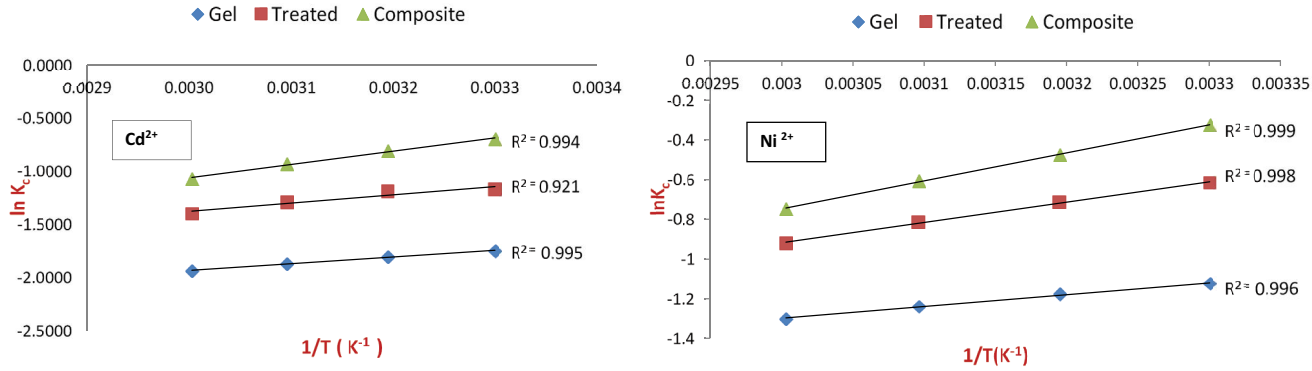

Fig. 14. Thermodynamic parameters of Cd^{2+} and Ni^{2+} ions by (Cs/Gltn/PDMAEMA)gel, T-(Cs/Gltn/PDMAEMA), and (Cs/Gltn/PDMAEMA-SiO_2)comp.

Table 4
Enthalpy ($\Delta H°$) and entropy ($\Delta S°$) for Cd^{2+} and Ni^{2+} ions

Items	Cs/Gltn/PDMAEMA		T-(Cs/Gltn/PDMAEMA)		Cs/Gltn/PDMAEMA/SiO_2)	
	Cd^{2+}	Ni^{2+}	Cd^{2+}	Ni^{2+}	Cd^{2+}	Ni^{2+}
$\Delta H°$ (kJ/mol)	–5.22	–4.95	–6.44	–8.50	–10.46	–11.71
$\Delta S°$ (J/mol)	–31.75	–25.63	–30.79	–33.14	–40.23	–41.35

Table 5
Evaluation of tannery wastewater treatment

Item	TDS, mg/L	COD	BOD	Color, %	Metal ions, mg/L	Turbidity, NTU	pH
Untreated	2,753	3,524	375	48	213	548	8.4
Treated	841	1,438	120	12	63	296	5.3
Removal (%)	69.5	59.2	65.6	75	70.4	46.2	–

Table 6
Chemical analysis of heavy metal ions in tannery wastewater

Effluent	Cr^{3+}	Zn^{2+}	Ni^{2+}	Pb^{2+}	Cu^{2+}	Cd^{2+}	As^{3+}	Total
Ionic radius (Å)	0.76	0.74	0.70	133	0.71	0.92	0.72	–
Untreated (mg/L)	151.9	16.9	14.0	11.0	9.1	8.0	1.99	213
Treated (mg/L)	50.9	5.0	2.7	1.7	1.2	0.89	0.59	63
Removal (%)	66.5	70.4	80.7	84.6	86.8	88.9	70.4	70.4

of metal cations moreover the ionic radii. The Ni^{2+} content is 14.00 mg/L and the removal percentage is 80.7%. Cd^{2+} content is 8.0 mg/L and the removal percentage is 88.9%. It may be indicated to some selectivity of this composite.

4. Conclusions

In this study, Cd^{2+} and Ni^{2+} ions were extracted from wastewater. For this purpose (Cs/Gltn/PDMAEMA-SiO_2) comp was prepared by gamma irradiation. The properties of the prepared composite were done and compared with the parent and treated gel. The adsorption study towards Cd^{2+} and Ni^{2+} was studied. The best adsorption was performed at pH5, 240 min contact time, and 10 g/L adsorbent dose. The adsorption of Ni^{2+} is higher than Cd^{2+} suggested the possible selectivity towards Ni^{2+}. (Cs/Gltn/PDMAEMA-SiO_2)comp has the highest value of adsorption capacity result from the presence of SiO_2 in the composite compared with the hydrogel and the treated one. The sorption capacity improves as the concentration of Ni^{2+} and Cd^{2+} is increased. However, the removal percentage decreased. The sorption capacity and the removal percentage decrease as the temperature is increased. The pseudo-second-order rate expression fit well the experimental data. Therefore, a chemical reactions may be included in the adsorption process. The Freundlich isotherm model fit well equilibrium adsorption data. The composite was tested for tannery wastewater. It was found a different trend from our experimental results.

References

[1] R. Singh, N. Gautam, A. Mishra, R. Gupta, Heavy metals and living systems: an overview, Indian J. Pharmacol., 43 (2011) 246–253.
[2] F. Burke, S. Hamza, S. Naseem, S. Nawaz-ul-Huda, M. Azam, I. Khan, Impact of cadmium polluted groundwater on human health: winder, Balochistan, SAGE Open, 6 (2016), doi: 10.1177/2158244016634409.
[3] R. Usatine, M. Riojas, Diagnosis and management of contact dermatitis, Am. Fam. Physician, 82 (2010) 249–255.
[4] W.W. Ngah, M.M. Hanafiah, Removal of heavy metal ions from wastewater by chemically modified plant wastes as adsorbents: a review, Bioresour. Technol., 99 (2008) 3935–3948.
[5] F. Fu, Q. Wang, Removal of heavy metal ions from wastewaters: a review, J. Environ. Manage., 92 (2011) 407–418.
[6] W.W. Ngah, L. Teong, M. Hanafiah, Adsorption of dyes and heavy metal ions by chitosan composites: a review, Carbohydr. Polym., 83 (2011) 1446–1456.
[7] A. Sowmya, S. Meenakshi, Effective removal of nitrate and phosphate anions from aqueous solutions using functionalised chitosan beads, Desal. Water Treat., 52 (2014) 2583–2593.
[8] H.N. Bhatti, Y. Safa, S.M. Yakout, O.H. Shair, M. Iqbal, A. Nazir, Efficient removal of dyes using carboxymethyl cellulose/alginate/polyvinyl alcohol/rice husk composite: adsorption/desorption, kinetics and recycling studies, Int. J. Biol. Macromol., 150 (2020) 861–870.
[9] J. Liu, Y. Chen, T. Han, M. Cheng, W. Zhang, J. Long, X. Fu, A biomimetic SiO_2@chitosan composite as highly-efficient adsorbent for removing heavy metal ions in drinking water, Chemosphere, 214 (2019) 738–742.
[10] V. Van Tran, D. Park, Y.-C. Lee, Hydrogel applications for adsorption of contaminants in water and wastewater treatment, Environ. Sci. Pollut. Res., 25 (2018) 24569–24599.
[11] W. Wu, J. Liu, S. Cao, H. Tan, J. Li, F. Xu, X. Zhang, Drug release behaviors of a pH sensitive semi-interpenetrating polymer network hydrogel composed of poly(vinyl alcohol) and star poly [2-(dimethylamino) ethyl methacrylate], Int. J. Pharm., 416 (2011) 104–109.
[12] C. Gao, M. Liu, S. Chen, S. Jin, J. Chen, Preparation of oxidized sodium alginate-graft-poly((2-dimethylamino) ethyl methacrylate) gel beads and *in vitro* controlled release behavior of BSA, Int. J. Pharm., 371 (2009) 16–24.
[13] M.S. Muhamad, M.R. Salim, W.-J. Lau, Preparation and characterization of PES/SiO_2 composite ultrafiltration membrane for advanced water treatment, Korean J. Chem. Eng., 32 (2015) 2319–2329.
[14] J. Liu, F. Chen, Q. Yao, Y. Sun, W. Huang, R. Wang, B. Yang, W. Li, J. Tian, Application and prospect of graphene and its composites in wastewater treatment, Pol. J. Environ. Stud., 29 (2020) 3965–3974.
[15] Z. Jing, Z. Guang-Yu, S. Dong-Xia, Review of graphene-based strain sensors, Chin. Phys. B, 22 (2013), doi: 10.1088/1674-1056/22/5/057701.
[16] M.A. Khalek, G.A. Mahmoud, E.M. Shoukry, M. Amin, A.H. Abdulghanyc, Adsorptive removal of nitrate ions from aqueous solution using modified biodegradable-based hydrogel, Desal. Water Treat., 155 (2019) 390–401.
[17] G. Mahmoud, M. Abdel Khalek, E. Shoukry, M. Amin, A. Abdulghany, Removal of phosphate ions from wastewater by treated hydrogel based on chitosan, Egypt. J. Chem., 62 (2019) 1537–1549.

[18] B. Liu, X. Peng, W. Chen, Y. Li, X. Meng, D. Wang, G. Yu, Adsorptive removal of patulin from aqueous solution using thiourea modified chitosan resin, Int. J. Biol. Macromol., 80 (2015) 520–528.
[19] G.A. Mahmoud, S.E. Abdel-Aal, N.A. Badway, A. Elbayaa, D.F. Ahmed, A novel hydrogel based on agricultural waste for removal of hazardous dyes from aqueous solution and reuse process in a secondary adsorption, Polym. Bull., 74 (2017) 337–358.
[20] A. Eaton, L. Clesceri, A. Greenberg, Standard Methods for the Examination of Water and Wastewater, American Public Health Association (APHA), Washington, DC, 2005, pp. 20001–23710.
[21] S. Chatterjee, M.W. Lee, S.H. Woo, Adsorption of congo red by chitosan hydrogel beads impregnated with carbon nanotubes, Bioresour. Technol., 101 (2010) 1800–1806.
[22] A.d.M.F. Guimarães, V.S.T. Ciminelli, W.L. Vasconcelos, Smectite organofunctionalized with thiol groups for adsorption of heavy metal ions, Appl. Clay Sci., 42 (2009) 410–414.
[23] A.A. Mohamed, G.A. Mahmoud, M.E. El Din, E. Saad, Synthesis and properties of (gum acacia/polyacryamide/SiO_2) magnetic hydrogel nanocomposite prepared by gamma irradiation, Polym. Plast. Technol. Mater., 59 (2020) 357–370.
[24] M. El-Barghouthi, A.A. Eftaiha, I. Rashid, M. Al-Remawi, A. Badwan, A novel super disintegrating agent made from physically modified chitosan with silicon dioxide, Drug Dev. Ind. Pharm., 34 (2008) 373–383.
[25] T. Bohli, I. Villaescusa, A. Ouederni, Comparative study of bivalent cationic metals adsorption Pb(II), Cd(II), Ni(II) and Cu(II) on olive stones chemically activated carbon, Chem. Eng. Technol., 4 (2013) 1–7.
[26] S. Hokkanen, E. Repo, T. Suopajärvi, H. Liimatainen, J. Niinimaa, M. Sillanpää, Adsorption of Ni(II), Cu(II) and Cd(II) from aqueous solutions by amino modified nanostructured microfibrillated cellulose, Cellulose, 21 (2014) 1471–1487.
[27] W. Wang, Y. Kang, A. Wang, One-step fabrication in aqueous solution of a granular alginate-based hydrogel for fast and efficient removal of heavy metal ions, J. Polym. Res., 20 (2013), doi: 10.1007/s10965-013-0101-0.
[28] G.A. Mahmoud, E. Hegazy, N.A. Badway, K.M.M. Salam, S. Elbakery, Radiation synthesis of imprinted hydrogels for selective metal ions adsorption, Desal. Water Treat., 57 (2016) 16540–16551.
[29] M.A. El-Latif, A.M. Ibrahim, M. El-Kady, Adsorption equilibrium, kinetics and thermodynamics of methylene blue from aqueous solutions using biopolymer oak sawdust composite, Am. J. Sci., 6 (2010) 267–283.
[30] R. Laus, T.G. Costa, B. Szpoganicz, V.T. Fávere, Adsorption and desorption of Cu(II), Cd(II) and Pb(II) ions using chitosan crosslinked with epichlorohydrin-triphosphate as the adsorbent, J. Hazard. Mater., 183 (2010) 233–241.
[31] S.P. Kamble, S. Jagtap, N.K. Labhsetwar, D. Thakare, S. Godfrey, S. Devotta, S.S. Rayalu, Defluoridation of drinking water using chitin, chitosan and lanthanum-modified chitosan, Chem. Eng. J., 129 (2007) 173–180.
[32] H.C. Man, W.H. Chin, M.R. Zadeh, M.R.M. Yusof, Adsorption potential of unmodified rice husk for boron removal, BioResources, 7 (2012) 3810–3822.
[33] S. Kaur, S. Rani, R.K. Mahajan, Adsorption kinetics for the removal of hazardous dye congo red by biowaste materials as adsorbents, J. Chem., 2013 (2012), doi: 10.1155/2013/628582.
[34] P.T. Jagung, Removal of Zn(II), Cd(II) and Mn(II) from aqueous solutions by adsorption on maize stalks, J. Anal. Sci., 15 (2011) 8–21.
[35] E. Khozamy, G. Mahmoud, E. Saad, S. Serror, Implementation of carboxymethyl cellulose/acrylic acid/titanium dioxide nanocomposite hydrogel in remediation of Cd(II), Zn(II) and Pb(II) for water treatment application, Egypt. J. Chem., 62 (2019) 1785–1798.
[36] A. de Sá, A.S. Abreu, I. Moura, A.V. Machado, Polymeric materials for metal sorption from hydric resources, Water Purif., (2017) 289–322, doi: 10.1016/B978-0-12-804300-4.00008-3.
[37] N. Oladoja, C. Aboluwoye, Y. Oladimeji, Kinetics and isotherm studies on methylene blue adsorption onto ground palm kernel coat, Turk. J. Eng. Environ. Sci., 32 (2009) 303–312.
[38] T. Benzaoui, A. Selatnia, D. Djabali, Adsorption of copper(II) ions from aqueous solution using bottom ash of expired drugs incineration, Adsorpt. Sci. Technol., 36 (2018) 114–129.